LME-MPM applied to quasi-brittle fracture.

Miguel Molinos[a1], Pedro Navas[a2], Diego Manzanal[a], and Manuel Pastor[a]

[a] *ETSI Caminos, Canales y Puertos, Universidad Politéctnica de Madrid. c. Prof. Aranguren 3, 28040 Madrid, Spain*

Abstract

The objective of this work is to introduce an alternative technique to address the fracture process of brittle and quasi-brittle materials under the Material Point Method (MPM) framework. With this purpose the eigensoftening algorithm, developed originally for the Optimal Transportation Meshfree (OTM) approximation scheme, is extended to the MPM with the aim of present a suitable alternative to the existing fracture algorithms developed for the MPM. The good fitting in the predictions made by the eigensoftening algorithm against both analytical and experimental results proofs the well performance of the method under challenging loads.

Keywords: Quasi brittle fracture, Local-*max-ent* approximation, Material Point Method, Solid Dynamics

1. Introduction

Presence of cracks are a violation of the continuity requirement in Finite Element Method (FEM). To overcome it, numerous of numerical artifacts has been proposed with the aim of reproducing such a complex behaviour. These techniques vary from employing cohesive approaches [1, 2], by adaptively inserting cohesive elements [3, 4, 5] at solid elements boundaries, or handling arbitrary cracks paths by level set representation of the fracture surface [6]. The simulation of fracture propagation in a more accurate and effective way can be considered as one of the original drivers for developing novel spatial discretization methods like meshfree techniques. Some examples of it are the Material Point Method (MPM) [7, 8, 9, 10], the Element-Free Galerkin Method (EFGM) [11, 12, 13, 14], the Smoothed Particle Hydrodynamics (SPH) [15, 16], the Optimal Transportation Meshfree (OTM) [17, 18, 19, 20]

[1]Corresponding author: m.molinos@alumnos.upm.es
[2]Corresponding author: p.navas@upm.es

or Peridynamics [21, 22] among others.

Regarding MPM, fracture can be described numerically in two ways. One is the "CRAcks with Material Points (CRAMP)" [9, 23] and consist in to remove the restriction of the single-valued velocity field close to the crack thorough two or more sets of nodes. In this method, different labels are assigned to the material points and nodes to distinguish if they are in the same side of the crack or not. Under this approach crack surface is described with line segments in 2D and triangle patches in 3D cases. The chosen criteria for crack propagation is based on such parameters as energy release rate analyzed by Tan & Nairn (2002)[24], and the stress intensity factor or the J-integral discussed by Guo & Nairn (2004)[25]. The other approach is to introduce failed material points to describe the crack evolution. In this method, the formation of failed points describes the nucleation of cracks, and thereafter its propagation and branching. Consequently, the position of the crack does not need to be explicitly stated. These represents significant advantages over the "CRAMP". Under this approach, the prediction of failure evolution is computed with a decohesion model, which has been discussed by Chen *et al.*[10] and Schreyer *et al.*[7]. And has been successfully employed to simulate the fracture of brittle materials by Chen *et al.* [8, 26] and Sulsky & Schreyer [27].

Similar to this approach, Schmidt *et al.* [28] introduced the concept of eigenfracture, where they approximate the crack set by means of eigendeformations, wich enable the material to develop displacement jumps at no cost of local elastic energy. Later, the eigenerosion approach to brittle facture was developed by Pandolfi *et al.* [29, 19]. In this technique the erosion of the material point means that each material point can be either intact or be completely failed or eroded and has no load bearing capacity. This method has been successfully applied to simulate high complex phenomena such dynamic fragmentation of metals [20]. Recently, Zhang *et al.* [30] adopted the eigenerosion to resolve the dynamic fracture of brittle materials in the MPM framework. Nonetheless, in quasi-brittle materials simulations performed with this approach exhibit an overestimation of tensile stress and the strain peaks. And conventional MPM/GIMP always faces stress oscillations.

To overcome the limitations observed in the EigenMPM [30]. The present research propose the eigensoftening algorithm developed by Navas *et al.* [31, 32] for the OTM framework and engineered for quasi-brittle materials. Inspired in the concept of the crack band model [33], since energy dissipation is thorough the softened (or failed) volume, it is able to capture the gradual rather than abrupt dissipation of the fracture energy. Second, to

mitigate stress oscillations the Local Maximum-Entropy (LME) approximation technique [34] to deal with tensile instabilities, such those that occurs when particles crosses an element boundary.

The paper is structured as follows. First meshfree methodology, eigenerosion and eigensoftening algorithms are presented in Section 2. Then, both approaches are compared and verified by means of comparisons with analytical and experimental results in Section 3. Finally, relevant conclusions are exposed in Section 4.

2. The meshfree methodology

The aim of this section is to provide an overview of the special techniques employed to face the fracture problem under the MPM framework. In consequence it is structured as follows: first in 2.1 the Newmark Predictor-Corrector (NPC) algorithm for the MPM will be exposed, next the LME approximants are introduced in 2.2 as an accurate alternative technique to interpolate data between particles and nodes, and finally fracture algorithms based in the eigendeformation concept are presented in 2.3.

2.1. The MPM time integration : A Newmark Predictor-Corrector scheme

The MPM [35] is a meshfree Lagrangian-Eulerian method where moving material points, henceforth particles, carries on all the physical information of the local state $(\sigma_p, \varepsilon_p)$ and a set of fixed background nodes is employed to compute the balance of momentum equation. Since the MPM possesses the advantages of both Lagrangian and Eulerian descriptions, no element distortion takes place in the MPM. Therefore it is an appropriate and efficient method to solve problems with moving discontinuities such as fracture evolution.

Without loosing generality, the MPM algorithm can be described with three main steps: (i) a variational recovery process, where particle data is projected to the grid nodes, (ii) an Eulerian step, where balance of momentum equation is expressed as a nodal equilibrium equation in a FEM-like procedure, and finally (iii) a Lagrangian advection of the particles. In the present research a explicit predictor-corrector time integration scheme is adopted. The purposes of this choice is motivated due its proved robustness and stability for dynamic computations. In the first stage, the nodal velocity predictor is computed following (1),

$$\tilde{\vec{v}}_I^{k+1} = \frac{N_{Ip}^k m_p (\vec{v}_p^k + (1-\gamma)\ \Delta t\ \vec{a}_p^k)}{\mathbf{m}_I^{k+1}}\ . \tag{1}$$

This way of computing the nodal predictor is both numerically stable and minimise the computational effort. Once nodal velocities are obtained, the essential boundary conditions are imposed. After that, a Eulerian phase is computed in the set of nodes in a FEM-like way, where nodal forces $\vec{f}_I^{k+1}$ are computed thorough the equilibrium equation. Next the nodal velocities are corrected in a *corrector* stage,

$$\vec{v}_I^{k+1} = \vec{v}_I^{pred} + \gamma \ \Delta t \ \frac{\vec{f}_I^{k+1}}{\mathbf{m}_I^{k+1}} \ . \tag{2}$$

Finally updated the particles are advected in the Lagrangian stage as

$$\vec{a}_p^{k+1} = \frac{N_{Ip}^k \vec{f}_I^k}{\mathbf{m}_I^k} \ , \tag{3}$$

$$\vec{v}_p^{k+1} = \vec{v}_p^n + \Delta t \ \frac{N_{Ip}^k \ \vec{f}_I^k}{\mathbf{m}_I^k} \ , \tag{4}$$

$$\vec{x}_p^{k+1} = \vec{x}_p^n + \Delta t \ N_{Ip}^k \ \vec{v}_I^k + \frac{1}{2}\Delta t^2 \ \frac{N_{Ip}^k \ \vec{f}_I^k}{\mathbf{m}_I^k} \ . \tag{5}$$

The complete pseudo-algorithm it is summarised in Appendix A.

2.2. Spatial interpolation technique : Local Maximum-Entropy approximants

Local Maximum-Entropy (LME) approximation scheme was introduced by Arroyo & Ortiz (2006)[34] as a bridge between finite elements and meshfree methods. The key idea under this interpolation technique is the interpretation of each nodal value N_I as a probability. Related with this definition, two important limits are introduced. First the maximum-entropy (*max-ent*) limit, which ensures a *unbiased statistical inference* based on the nodal data as states the Jayne's[36] principle of *maximum entropy*. And second the Delaunay triangulation that warranties the *least width* shape function support. To reach to a compromise between two competing objectives, a Pareto set is defined as,

$$\text{(LME)}_\beta \text{ For fixed } \vec{x} \text{ minimise } f_\beta(\vec{x}_p, N_I) \coloneqq \beta U(\vec{x}_p, N_I) - H(N_I)$$

$$\text{subject to } \begin{cases} N_I \geq 0, \ \text{I=1, ..., n} \\ \sum_{I=1}^{N_n} N_I = 1 \\ \sum_{I=1}^{N_n} N_I \vec{x}_I = \vec{x} \end{cases}$$

where $H(N_I)$ is the entropy of the system of nodes following the definition given by Shannon (1948) [37], the shape function width is defined as $U(\vec{x}_p, N_I) \coloneqq \sum_I N_I |\vec{x}_p - \vec{x}_I|^2$, and β is a regularization o *thermalization* parameter such that for Pareto optimal solutions $\beta \in (0, \infty)$. Notice that β has units of $[L]^{-2}$, therefore it can be controlled by adjusting a dimensionless parameter, $\gamma = \beta h^2$ [34], where h is defined as a suitable measure of the nodal spacing. With the restrictions exposed in (**??**), the unique solution of the local *max-ent* problem LME_β is,

$$N_I^*(\vec{x}) = \frac{\exp\left[-\beta\ |\vec{x} - \vec{x}_I|^2 + \vec{\lambda}^* \cdot (\vec{x} - \vec{x}_I)\right]}{Z(\vec{x}, \vec{\lambda}^*)}, \tag{6}$$

where $Z(\vec{x}, \vec{\lambda}^*)$ is the *partition function* defined as,

$$Z(\vec{x}, \vec{\lambda}) = \sum_{I=1}^{N_n} \exp\left[-\beta\ |\vec{x} - \vec{x}_I|^2 + \vec{\lambda} \cdot (\vec{x} - \vec{x}_I)\right], \tag{7}$$

and a Lagrange multiplier $\vec{\lambda}^*$ such minimise the function $\log Z(\vec{x}, \vec{\lambda})$. The traditional way to compute the optimal value of $\vec{\lambda}^*$ is thorough a Newton-Raphson procedure, or in more challenging scenarios by a combination of the Newton-Raphson and the Nelder-Mead Simplex algorithms [32]. Nonetheless, since finite strains are not involved in the present research, Newton-Raphson is an enough efficient method. For an uniform nodal spacing, β can be considered constant, thus first derivatives of the interpolation technique ∇N_I^* can be obtained by evaluating the following expression

$$\nabla N_I^* \ = \ -N_I^* \left(\mathbf{J}^*\right)^{-1} (\vec{x} - \vec{x}_I) \tag{8}$$

where $\mathbf{J}$ is the Hessian matrix, defined by

$$\mathbf{J}(\vec{x}, \vec{\lambda}, \beta) \ \equiv \ \frac{\partial \vec{r}}{\partial \vec{\lambda}}, \tag{9}$$

$$\vec{r}(\vec{x}, \vec{\lambda}, \beta) \ \equiv \ \frac{\partial \log Z(\vec{x}, \vec{\lambda})}{\partial \vec{\lambda}} = \sum_I^{N_n} p_I(\vec{x}, \vec{\lambda}, \beta)\, (\vec{x} - \vec{x}_I). \tag{10}$$

An additional remark concerning the support of the interpolation function is that in practice the value of N_I decay exponentially following $\exp(-\beta\vec{r})$. In this sense a good practice is to truncate it under a tolerance, 10^{-6} would ensure a reasonable range of neighbours, see [34] for details. This tolerance defines a limit value of the influence radius to find the neighbour nodes of a given integration point.

2.3. Fracture modelling approach

Within the context of MPM formulation, fracture can be modelled by failing particles according to a suitable failure criterion. When material points are failed, they are assumed to have null stress tensor. To reproduce this behaviour in the present research, the eigensoftening algorithm is introduced in the MPM framework as an alternative approach to the decohesion model [10, 7]. The eigensoftening concept was originally developed by Navas *et al.* (2017)[31] as an extension for quasi-brittle materials of the eigenerosion proposed by Pandolfi & Ortiz (2012)[29] for fracture of brittle materials. A comparison between both in [31] shows that the eigenerosion algorithm significantly overestimates the tensile stress and the strain peaks, while it captures the forces and crack patterns accurately. On the other hand eigensoftening algorithm agree very well with experimental results in all the aspects. Furthermore, this algorithm has proof its accuracy for complex fracture patters such the present in fiber reinforces concrete (FRC), [38].

The key idea behind the eigenerosion algorithm is the computation of the energy-release rate attendant to the failure of material point p,

$$G_p^{k+1} = \frac{C_\epsilon}{m_p^{k+1}} \sum_{x_q^{k+1} \in B_\epsilon(x_p^{k+1})} m_q W_q^{k+1} \tag{11}$$

$$m_p^{k+1} = \sum_{x_q^{k+1} \in B_\epsilon(x_p^{k+1})} m_q \tag{12}$$

where $B_\epsilon(x_p^{k+1})$ is a ^{n}dimensional sphere of radius ϵ centered at x_p^{k+1}. The particles which lies under this sphere are known as the ϵ-neighborhood of the material point, see [29], this concept is conveniently is sketched in Figure 1. Other parameters are, the mass of the neighborhood m_p^{k+1}, the current free-energy density per unit mass W_q^{k+1} and finally a normalizing constant C_ϵ. The failure criterion consist in to consider the material point fails when G_p^{k+1} surpasses a critical energy release rate that measures the material-specific energy, G_F. The convergence of this approach has been analyzed by Schmidt *et al.* (2009)[28], who proofed that it converges to the Griffith fracture when discretization size tends to zero. It is necessary to point out that when a material point overpass the critical energy, its contribution to the internal forces vector is set to zero, but its contribution to the mass matrix is preserved.

As can be noticed, the eigenerosion algorithm relies over an energetic failure criterion. Because of this, unrealistic stress concentration (higher than tensile strength) appears in quasi-brittle materials [31]. To overcome this limitation, the aforementioned authors proposed the concept of eigensoftening

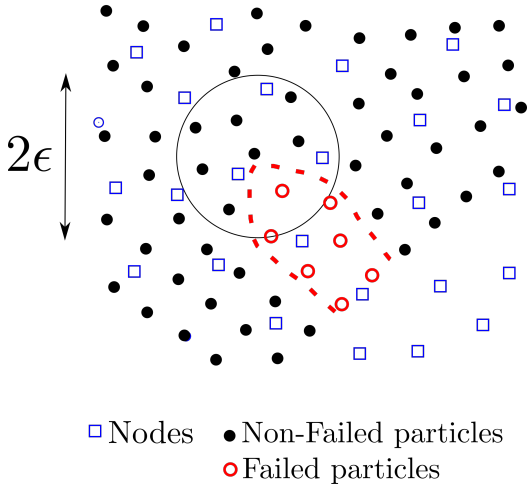

Figure 1: Scheme of a linear cohesive law, where the shaded area is G_f, f_t is the tensile strength, and w_c is the critical opening displacement.

to take in to account the gradual failure in quasi-brittle materials. The idea behind this concept is inspired in the cohesive fracture. This gradual failure criterion is plotted in figure , where a linear decreasing cohesive law is presented to illustrate the concept earlier described. In the picture, the shaded region represents the static fracture energy per unit of area, G_F. Notice how a cohesive crack appears when the maximum tensile strength, f_t is reached. Once the opening displacement w reach the value of the critical crack displacement w_c, a stress-free crack is attained. For intermediate values, w_n, a damage value between zero and one represents the extension to which the material has failed. For the eigensoftening algorithm, a strength criterion for crack initialization was adopted. Particularly the maximum principal stress theory for brittle fracture was considered by authors [31]. With that purpose, the variation of the averaged strain energy density in the ϵ-neighborhood of the material point $\vec{x}_p^{k+1}$ can be obtained as

$$\delta W_{\epsilon,p} = \frac{\partial G_p}{C_\epsilon} = \frac{1}{m_p} \sum_{x_q^{k+1} \in B_\epsilon(x_p^{k+1})} m_q \sigma_{q,I} \delta\epsilon_q, \tag{13}$$

where $\sigma_{q,I}$ is the maximum principal stress of each material point in the ϵ-neighborhood. In this point in introduced an effective strain ε_q, such the variation of the local strain energy can be obtained as $\delta W_q = \sigma_{q,1}\delta\varepsilon_q$. Now with the assumption that the effective strain of each material point at every time step is constant in the neighborhood of $\vec{x}_p^{k+1}$, the equation (13) can be

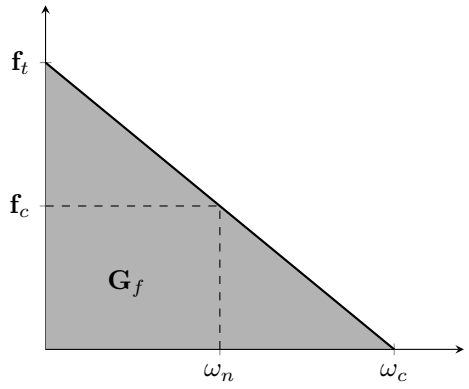

Figure 2: Scheme of a linear cohesive law, where the shaded area is G_f, f_t is the tensile strength, and w_c is the critical opening displacement.

simplified to

$$\delta W_{\epsilon,p} = \frac{\delta \epsilon_p}{m_p} \sum_{x_q^{k+1} \in B_\epsilon(x_p^{k+1})} m_q \sigma_{q,I}. \tag{14}$$

Consequently it is possible to define an equivalent critical stress at the material point $\vec{x}_p^{k+1}$as

$$\sigma_{\epsilon,p} = \frac{1}{m_p} \sum_{x_q^{k+1} \in B_\epsilon(x_p^{k+1})} m_q \sigma_{q,I}, \tag{15}$$

where m_p is the total mass of the ϵ-neighborhood

$$m_p = \sum_{x_q^{k+1} \in B_\epsilon(x_p^{k+1})} m_q. \tag{16}$$

This definition of the equivalent critical stress leads to a definition of the averaged strain energy in terms of the averaged strain as $\delta W_{\epsilon,p} = \sigma_{\epsilon,p}\ \delta\varepsilon_p$. The softening behaviour is activated once $\sigma_{\epsilon,p}^{k+1}$ surpasses the tensile strength, f_t. This consists in a reduction of the internal forces as,

$$f_I^{int} = \sum_p (1 - \chi_p)\ \sigma_p^{k+1} \cdot grad(N_{Ip})\ \Omega_p \tag{17}$$

where χ_p and Ω_p are respectively the damage or softening variable and the volume for each material point p. χ_p takes values between zero (an intact

material) and one (completely failed material points). For the case of a linear softening such the sketched in the Figure 2, χ_p is computed as,

$$1 - \chi = \frac{f_n}{f_t} = 1 - \frac{w_n}{w_c} \;\rightarrow\; \chi = \frac{w_n}{w_c}. \tag{18}$$

In analogy to the band crack model presented by Bazant [33], Navas *et al.* [38] [31] introduced a band width parameter h_ϵ. Concerning this parameter, a typical value of it is between two and four times the maximum size of the aggregates, in the case of concrete as brittle material. The effective fracture strain $\varepsilon_{\epsilon,f}$ is defined as the difference between the strain at crack initialization, $\varepsilon_1(\vec{x}_p^0)$, and the current strain, $\varepsilon_1(\vec{x}_p^{k+1})$, for material point p. Also, $\varepsilon_{\epsilon,f}$ can be represented as the current crack opening w_n within the band width, h_ϵ. Therefore,

$$\varepsilon_{\epsilon,f} = \varepsilon_1(\vec{x}_p^{k+1}) - \varepsilon_1(\vec{x}_p^0) = \frac{w_n}{h_\epsilon} \tag{19}$$

Introducing (19) in (18), the damage variable can be computed as,

$$\chi = \frac{\varepsilon_{\epsilon,f}\ h^\epsilon}{w_c}. \tag{20}$$

The function of χ presented in (21) represents a linear softening behaviour. For a general case, the damage variable can be expressed in terms of the following variables,

$$\chi = \chi(\varepsilon_{\epsilon,f}, h^\epsilon, f_t, w_c, G_f) \tag{21}$$

3. Cases of study and discussion

As noticed in [30], the EigenMPM have two important shortcomings. The first is the presence of stress instabilities even with GIMP shape functions. To overcome it, LME approximants are introduced as an alternative to the existing interpolation techniques. Its impressive performance mitigating spurious stress oscillations [39] under the MPM framework help to enhance notoriously the quality of the results as we can see in Section 3.1. Where both interpolation techniques are compared by carry out an eigenerosion simulation. The second limitation is concerning its inability to simulate properly quasi-brittle fracture [38]. It can be solved thorough the eigensoftening algorithm described in Section 2.3. A proof of it is exposed in Section 3.2, where experimental results of a drop-weight impact test are compared with those produced by eigensoftening computations.

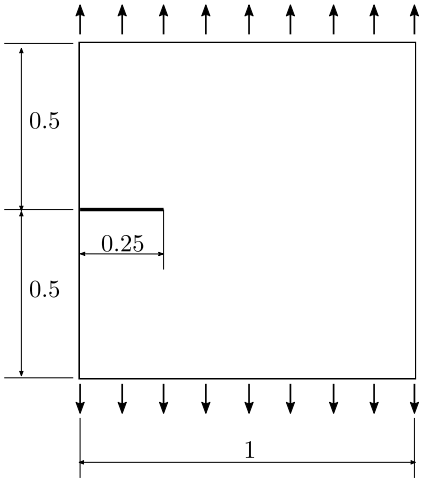

Figure 3: Geometry and boundary condition of the drop-weight impact test.

3.1. Edge-cracked square panel in mode I

This problem here presented is devoted to compare how much LME approximants are able to improve the result *versus* standard linear interpolation. It consists in a square plate of size $H = 1$ containing an initial edge crack of length $0.25 \cdot H$ loaded in a pure mode I by displacement control on the outer flanks of the plate, Figure 3. The constitutive model consider for numerical experiment is a linear-elastic Hookean material, where Young's modulus $E = 1.06$, the Poisson's ratio $\mu = 0.333$, and critical energy-release rate $G_c = 0.0001$.

Figure 4 clearly shows the presence of wiggles in the loading and also in the unloading regions of the curve when a linear interpolation technique is employed. In contrast with it LME simulation does not exhibit this accuracy and remains rectilinear during loading and unloading. An important consideration regarding the presence of oscillations once both parts of the panel are separated. Is that they should not be attributed to the eigenerosion algorithm since the fracture process is over. They are due to the dynamic nature of the simulation.

3.2. Drop-weight impact test

4. Conclusions

Acknowledgements

The financial support to develop this research from the Ministerio de Ciencia e Innovación, under Grant No. BIA-2016-76253 is greatly appreciated. The first and the second authors also acknowledge the fellowship

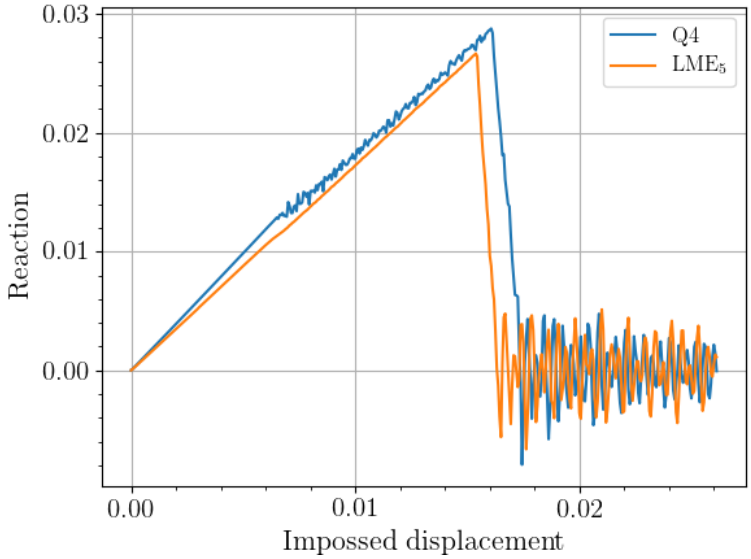

Figure 4: Evolution of the reaction forces plotted *versus* the imposed displacement for linear interpolation technique and the LME approximants.

155 Fundación Agustín de Betancourt and Juan de la Cierva (FJCI-201731544) respectively.

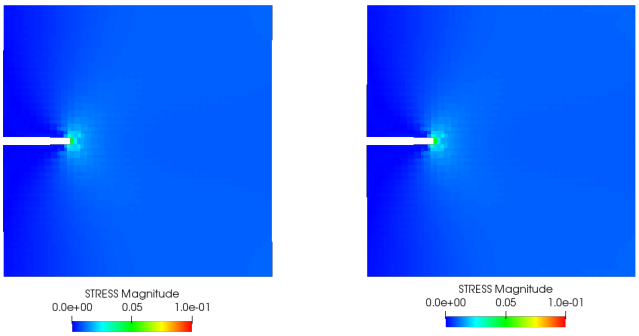

(a) t1

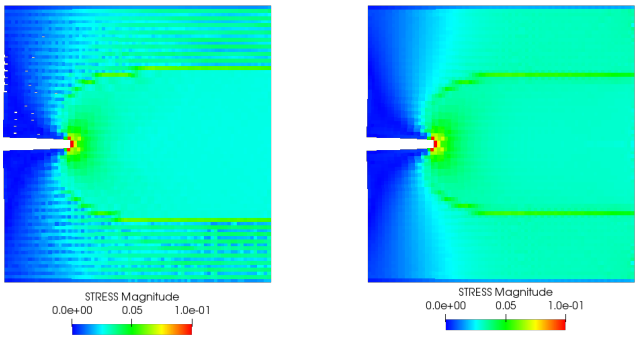

(b) t2

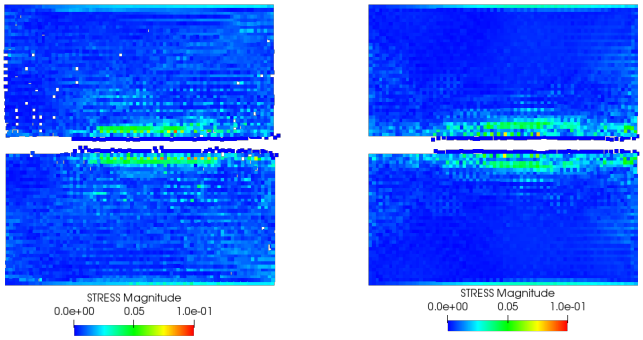

(c) t3

Figure 5: Evolution of the stress tensor magnitude for linear interpolation (pictures in the left side), and LME (pictures in the right side). Both simulations performed with an eigenerosion algorithm.

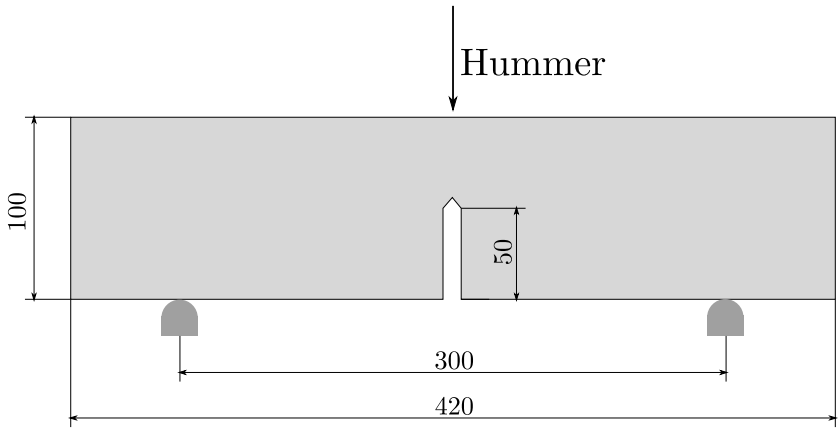

Figure 6: Geometry and boundary condition of the drop-weight impact test.

Appendix A. Explicit Predictor-Corrector algorithm

Appendix B. Eigensoftening Algorithm

References

[1] G. Barenblatt, The mathematical theory of equilibrium cracks in brittle fracture., Advances in Applied Mechanics 7 (1962) 55–129.

[2] A. Hillerborg, M. Modéer, P. Petersson, Analysis of crack formation and crack growth in concrete by means of fracture mechanics and finite elements., Cement and Concrete Research. 6 (1976) 773–782.

[3] M. Ortiz, A. Pandolfi, Finite-deformation irreversible cohesive elements for three-dimensional crack-propagation analysis., International Journal for Numerical Methods in Engineering. 44 (1999) 1267–1282.

[4] A. Pandolfi, M. Ortiz, An efficient adaptive procedure for three-dimensional fragmentation simulations., Engineering with Computers. 18(2) (2002) 148–159.

[5] G. Ruiz, M. Ortiz, A. Pandolfi, Three-dimensional finite-element simulation of the dynamic Brazilian tests on concrete cylinders, International Journal for Numerical Methods in Engineering 48 (2000) 963–994.

[6] T. Belytschko, H. Chen, J. Xu, G. Zi, Dynamic crack propagation based on loss of hyperbolicity and a new discontinuous enrichment., International Journal for Numerical Methods in Engineering. 58 (2003) 1873–1905.

[7]

[8] Z. Chen, W. Hu, L. Shen, X. An, R. Brannon, An evaluation of the mpm for simulating dynamic failure with damage diffusion, Engineering Fracture Mechanics 69 (2002) 1873–1890. doi:10.1016/S0013-7944(02)00066-8.

[9] J. Nairn, Material point method calculations with explicit cracks, Computer Modeling in Engineering & Sciences 4 (6) (2003) 649–664. doi:10.3970/cmes.2003.004.649.
URL http://www.techscience.com/CMES/v4n6/33290

[10] Z. Chen, L. Shen, Y.-W. Mai, Y.-G. Shen, A bifurcation-based decohesion model for simulating the transition from localization to decohesion with the mpm, Zeitschrift fur Angewandte Mathematik und Physik 56 (2005) 908–930. doi:10.1007/s00033-005-3011-0.

Algorithm 1: Explicit Predictor-Corrector scheme

1 [1] **Update mass matrix**:

$$\mathbf{m}_I = N_{Ip}^k \; m_p,$$

Explicit Newmark Predictor:

2

$$\vec{v}_I^{pred} = \frac{N_{Ip}^k m_p (\vec{v}_p^k + (1-\gamma) \; \Delta t \; \vec{a}_p^k)}{m_I}$$

Impose essential boundary conditions:

3 At the fixed boundary, set $\vec{v}_I^{pred} = 0$. **Deformation tensor increment calculation**.

$$\Delta\varepsilon_p^{k+1} = \Delta t \; \dot{\varepsilon_p}^{k+1} = \Delta \left[\vec{v}_I^{pred} \otimes grad(N_{Ip}^{k+1}) \right]^s$$

Update the density field:

$$\rho_p^{k+1} = \frac{\rho_p^k}{1 + tra \left[\Delta\varepsilon_p^{k+1} \right]}.$$

Compute stress field and update damage parameter:

4 **Balance of forces calculation**:

5 Calculate the total grid nodal force $\vec{f}_I^{k+1} = \vec{f}_I^{int,k+1} + \vec{f}_I^{ext,k+1}$.

Explicit Newmark Corrector:

6

$$\vec{v}_I^{k+1} = \vec{v}_I^{pred} + \gamma \; \Delta t \; \frac{\vec{f}_I^{k+1}}{\mathbf{m}_I^{k+1}}$$

Update particles lagrangian quantities:

$$\vec{a}_p^{k+1} = \frac{N_{Ip}^k \vec{f}_I^k}{\mathbf{m}_I^k}$$

$$\vec{v}_p^{k+1} = \vec{v}_p^n + \Delta t \; \frac{N_{Ip}^k \; \vec{f}_I^k}{\mathbf{m}_I^k}$$

$$\vec{x}_p^{k+1} = \vec{x}_p^n + \Delta t \; N_{Ip}^k \; \vec{v}_I^k + \frac{1}{2}\Delta t^2 \; \frac{N_{Ip}^k \; \vec{f}_I^k}{\mathbf{m}_I^k}$$

Reset nodal values

Algorithm 2: Compute damage parameter χ_p^{k+1}

For each p, ϵ-neighbourhood, $f_{t,p}$, $h_{\epsilon,p}$, w_c Return damage parameter $\chi := \{\chi_p\}$ $\chi_p \leftarrow \chi_p^k$
for p *to* N_p **do**
  if $\chi_p = 0$ $\epsilon_{f,p} = 0$ **then**
    for $q \in B_{\epsilon,p}$ **do**
      $\sigma_{q,I} \leftarrow$ getEigenvaluesOf(σ_q)
      if $\chi_q < 1$ **then**
        $\sum m_p \sigma_{p,I} \leftarrow \sum m_p \sigma_{p,I} + m_q \sigma_{q,I}$
      $m_p \leftarrow m_p + m_q$
    $\sigma_{p,\epsilon} \leftarrow \frac{1}{m_p} \sum m_p \sigma_{p,I}$
    if $\sigma_{p,\epsilon} > f_{t,p}$ **then**
      $\epsilon_{f,p} = \epsilon_{I,p}$
    else if $\chi_p \neq 1$ $\epsilon_{f,p} > 0$ **then**
      $\chi_p^{k+1} \leftarrow \min\left\{1, \max\{\chi_p^k, \frac{(\epsilon_{I,p} - \epsilon_{f,p})\ h_{\epsilon,p}}{w_c}\}\right\}$

[11] T. Belytschko, Y. Lu, L. Gu, M. Tabbara, Element-free galerkin methods for static and dynamic fracture, International Journal of Solids and Structures 32 (17) (1995) 2547 – 2570. doi:https://doi.org/10.1016/0020-7683(94)00282-2.
URL http://www.sciencedirect.com/science/article/pii/0020768394002822

[12] T. Belytschko, D. Organ, C. Gerlach, Element-free galerkin methods for dynamic fracture in concrete, Computer Methods in Applied Mechanics and Engineering 187 (3) (2000) 385 – 399. doi:https://doi.org/10.1016/S0045-7825(00)80002-X.
URL http://www.sciencedirect.com/science/article/pii/S004578250080002X

[13] X. Zhuang, C. Augarde, K. Mathisen, Fracture modeling using meshless methods and level sets in 3d: Framework and modeling, International Journal for Numerical Methods in Engineering 92 (2012) 969–998. doi:10.1002/nme.4365.

[14] N. Muthu, S. Maiti, B. Falzon, I. Guiamatsia, A comparison of stress intensity factors obtained through crack closure integral and other ap-

proaches using extended element-free galerkin method, Computational Mechanics 52. doi:10.1007/s00466-013-0834-y.

[15] Y. Wang, H. T. Tran, G. D. Nguyen, P. G. Ranjith, H. H. Bui, Simulation of mixed-mode fracture using sph particles with an embedded fracture process zone, International Journal for Numerical and Analytical Methods in Geomechanics n/a (n/a). arXiv:https://onlinelibrary.wiley.com/doi/pdf/10.1002/nag.3069, doi:10.1002/nag.3069.
URL https://onlinelibrary.wiley.com/doi/abs/10.1002/nag.3069

[16] Y. Wang, H. Bui, G. Nguyen, P. Ranjith, A new sph-based continuum framework with an embedded fracture process zone for modelling rock fracture, International Journal of Solids and Structures 159 (2019) 40–57. doi:10.1016/j.ijsolstr.2018.09.019.

[17] B. Li, F. Habbal, M. Ortiz, Optimal transportation meshfree approximation schemes for fluid and plastic flows, International Journal for Numerical Methods in Engineering 83 (12) (2010) 1541–1579. doi:10.1002/nme.2869.
URL http://doi.wiley.com/10.1002/nme.2869

[18] B. Li, A. Kadane, G. Ravichandran, M. Ortiz, Verification and validation of the optimal-transportation meshfree (otm) simulation of terminal ballistics., International Journal for Impact Engineering 42 (2012) 25–36.

[19] A. Pandolfi, B. Li, M. Ortiz, Modeling fracture by material-point erosion., International Journal of fracture 184 (2013) 3–16.

[20] B. Li, A. Pandolfi, M. Ortiz, Material-point erosion simulation of dynamic fragmentation of metals., Mechanics of Materials 80 (2015) 288–297.

[21] Y. D. Ha, F. Bobaru, Characteristics of dynamic brittle fracture captured with peridynamics, Engineering Fracture Mechanics 78 (6) (2011) 1156 – 1168. doi:https://doi.org/10.1016/j.engfracmech.2010.11.020.
URL http://www.sciencedirect.com/science/article/pii/S0013794410004959

[22] T. Rabczuk, H. Ren, A peridynamics formulation for quasi-static fracture and contact in rock, Engineering Geology 225

(2017) 42 – 48, special Issue: Characterisation of Fractures in Rock: from Theory to Practice (ROCKFRAC). doi:https://doi.org/10.1016/j.enggeo.2017.05.001.
URL http://www.sciencedirect.com/science/article/pii/S0013795217306907

[23] Y. GUO, J. Nairn, Three-dimensional dynamic fracture analysis using the material point method, Computer Modeling in Engineering Sciences 16.

[24] H. Tan, J. Nairn, Hierarchical, adaptive, material point method for dynamic energy release rate calculations, Computer Methods in Applied Mechanics and Engineering 191 (2002) 2123–2137. doi:10.1016/S0045-7825(01)00377-2.

[25] Y. GUO, J. Nairn, Calculation of j-integral and stress intensity factors using the material point method, CMES. Computer Modeling in Engineering Sciences 6.

[26] Z. Chen, R. Feng, X. An, L. Shen, A computational model for impact failure with shearinduced dilatancy, International Journal for Numerical Methods in Engineering 56 (2003) 1979 – 1997. doi:10.1002/nme.651.

[27] S. DL, L. Schreyer, Mpm simulation of dynamic material failure with a decohesion constitutive model, European Journal of Mechanics - A/Solids 23 (2004) 423–445. doi:10.1016/j.euromechsol.2004.02.007.

[28] B. Schmidt, F. Fraternali, M. Ortiz, Eigenfracture: an eigendeformation approach to variational fracture., SIAM J. Multiscale Model. Simul. 7 (2009) 1237–1266.

[29] A. Pandolfi, M. Ortiz, An eigenerosion approach to brittle fracture., International Journal for Numerical Methods in Engineering 92 (2012) 694–714.

[30] K. Zhang, S.-L. Shen, A. Zhou, Dynamic brittle fracture with eigenerosion enhanced material point method, International Journal for Numerical Methods in Engineering n/a (n/a). arXiv:https://onlinelibrary.wiley.com/doi/pdf/10.1002/nme.6381, doi:10.1002/nme.6381.
URL https://onlinelibrary.wiley.com/doi/abs/10.1002/nme.6381

[31] P. Navas, R. Yu, B. Li, G. Ruiz, Modeling the dynamic fracture in concrete: an eigensoftening meshfree approach, International Journal of Impact Engineering 113. doi:10.1016/j.ijimpeng.2017.11.004.

[32] P. Navas, S. López-Querol, R. C. Yu, M. Pastor, Optimal transportation meshfree method in geotechnical engineering problems under large deformation regime, International Journal for Numerical Methods in Engineeringdoi:10.1002/nme.5841.

[33] Z. Bažant, B. Oh, Crack band theory for fracture in concrete., Materials and Structures. 16 (1983) 155–177.

[34] M. Arroyo, M. Ortiz, Local maximum-entropy approximation schemes: A seamless bridge between finite elements and meshfree methods, International Journal for Numerical Methods in Engineeringdoi:10.1002/nme.1534.

[35] D. L. Sulsky, H. Schreyer, Z. Chen, A particle method for history-dependent materials, Computer Methods in Applied Mechanics and Engineering 118 (1) (1994) 179–196. doi:10.1016/0045-7825(94)90112-0.

[36] E. Jaynes, Information Theory and Statistical Mechanics, The Physical Review 106 (4) (1957) 620–630.

[37] C. E. Shannon, A Mathematical Theory of Communication, Bell System Technical Journaldoi:10.1002/j.1538-7305.1948.tb01338.x.

[38] P. Navas, R. Yu, G. Ruiz, Meshfree modeling of the dynamic mixed-mode fracture in frc through an eigensoftening approach, Engineering Structures 172. doi:10.1016/j.engstruct.2018.06.010.

[39] E. Wobbes, R. Tielen, M. Möller, C. Vuik, Comparison and unification of material-point and optimal transportation meshfree methods, Computational Particle Mechanicsdoi:10.1007/s40571-020-00316-7.